Computed Tomography of the Liver

DAVID H. STEPHENS,[1] PATRICK F. SHEEDY, II, ROBERT R. HATTERY, AND ROBERT L. MacCARTY

The diagnostic value of computed tomography (CT) of the liver depends on proper conduct of the examination, knowledgeable interpretation of findings, and an appreciation of the capabilities and limitations of the method. This report documents 10 months of experience with abdominal CT in more than 600 liver examinations using a system fast enough to eliminate respiratory motion. This experience supplied data on the CT appearance of the normal liver and its variations and of various hepatic abnormalities, on the conduct of the examination, including the appropriate use of contrast material, and on some of the problems that reduce the technical quality of the examination. CT was highly accurate, but not infallible, in detecting and defining space-occupying lesions and in detecting fatty infiltration; it was less helpful in detecting diffuse hepatic disease. In bile duct obstruction, CT displayed not only the dilated ducts but often the obstructing lesion.

Since the liver is a large solid organ of soft-tissue composition, it is uniquely suited to examination by computed tomography (CT). The ability of CT to reveal hepatic lesions in experimental as well as clinical settings has been well illustrated in recent investigations [1–8]. We report information acquired during our first 10 months of clinical experience with CT examinations of the liver.

Materials and Methods

During its first 10 months of operation, the body scanning unit was used in 1,120 patient examinations. Of the 798 abdominal-pelvic examinations performed during this period, 632 included at least a substantial part of the liver. Evaluation of the liver was the primary indication for 109 of the abdominal examinations and was an important consideration in most of the others.

The body scanning instrument used is an EMI prototype model. Each scan requires 20 sec and produces a cross-sectional reconstruction that represents a slice 13 mm thick. The results are displayed on a 320 X 320 matrix. Most patients can suspend respiration for the required scan time.

The conduct of the examination has undergone modification as we acquired experience. Examinations during the early months, though carefully planned in advance, usually were not reviewed before the patient's dismissal because of a long processing time. We now attempt to process and view the initial series of scans so that more informed determinations can be made about the adequacy of the examination and the need for additional measures such as administration of contrast material. Generally, the indication for intravenous contrast material has been suspicion of a liver mass that is not found on the initial series of scans. In the early months, conventional doses of standard urographic agents were most often used; however, for liver scans we prefer the higher dose of iodine provided by infusion agents such as 300 ml of 30% diatrizoate methylglucamine.

Scans are usually made at 1.5 cm intervals when the liver is one of the primary organs of interest and at 2 cm intervals when it is being surveyed as a more incidental part of the examination. A preliminary radiograph with an overlying radiopaque grid is obtained to help locate the region to be scanned and for comparison with CT findings.

Observations and Results

Normal Liver

The liver is the dominant feature on cross-sectional CT reconstruction of the upper third of the abdomen (fig. 1). The contour of the liver, though generally smooth, has several indentations and bulges. The liver is penetrated anteriorly by the fissure containing the falciform ligament and ligamentum teres and posteriorly by the fissure containing the gastrohepatic ligament and ligamentum venosum (figs. 1*B* and 1*C*). Classically considered the boundary between right and left lobes, these fissures do not correspond to the distribution of the branches of the portal triad (portal vein, hepatic artery, and bile duct) within the liver. According to newer designations based on vascular distribution, the division between the right and the left lobe corresponds to a line from the gallbladder fossa on the anterior visceral surface to the fossa for the vena cava posteriorly [9].

The size and shape of the left lobe are inconstant. The left lobe is usually small and flattened (fig. 1), but it may also be large and rounded (fig. 2*A*) or almost nonexistent (fig. 2*B*).

The form of the right lobe is more constant, but it too has variations. On the visceral surface of the right lobe (by the classic lobar designation) are two subdivisions of variable prominence: posteriorly, the caudate lobe, which lies between the fossa for the inferior vena cava and the fissure for the ligamentum venosum; and anteriorly, the quadrate lobe, which lies between the gallbladder fossa and the fissure for the ligamentum teres. On cross-sectional scans, the caudate lobe is at a higher level than the quadrate lobe (fig. 1). Riedel's lobe is a caudal extension of the lateral aspect of the right lobe extending below the right kidney, which may be seen in cross section. It occurs predominantly in women.

Normally, the radiographic density of liver parenchyma is at least as great as, and usually greater than, the density of the other solid organs of the upper abdomen (i.e., spleen, kidneys, and pancreas). The range of attenuation values among normal livers is wide (20–40 EMI units), but in any one patient the range is much narrower, resulting in a generally homogeneous appearance of hepatic parenchyma.

Visualization of intrahepatic vessels in the normal liver depends on the density of the parenchyma. The density of the liver is generally greater than that of intravascular

Received November 3, 1976; accepted December 23, 1976.

[1] All authors: Department of Diagnostic Roentgenology, Mayo Clinic and Mayo Foundation, Rochester, Minnesota 55901. Address reprint requests to D. H. Stephens.

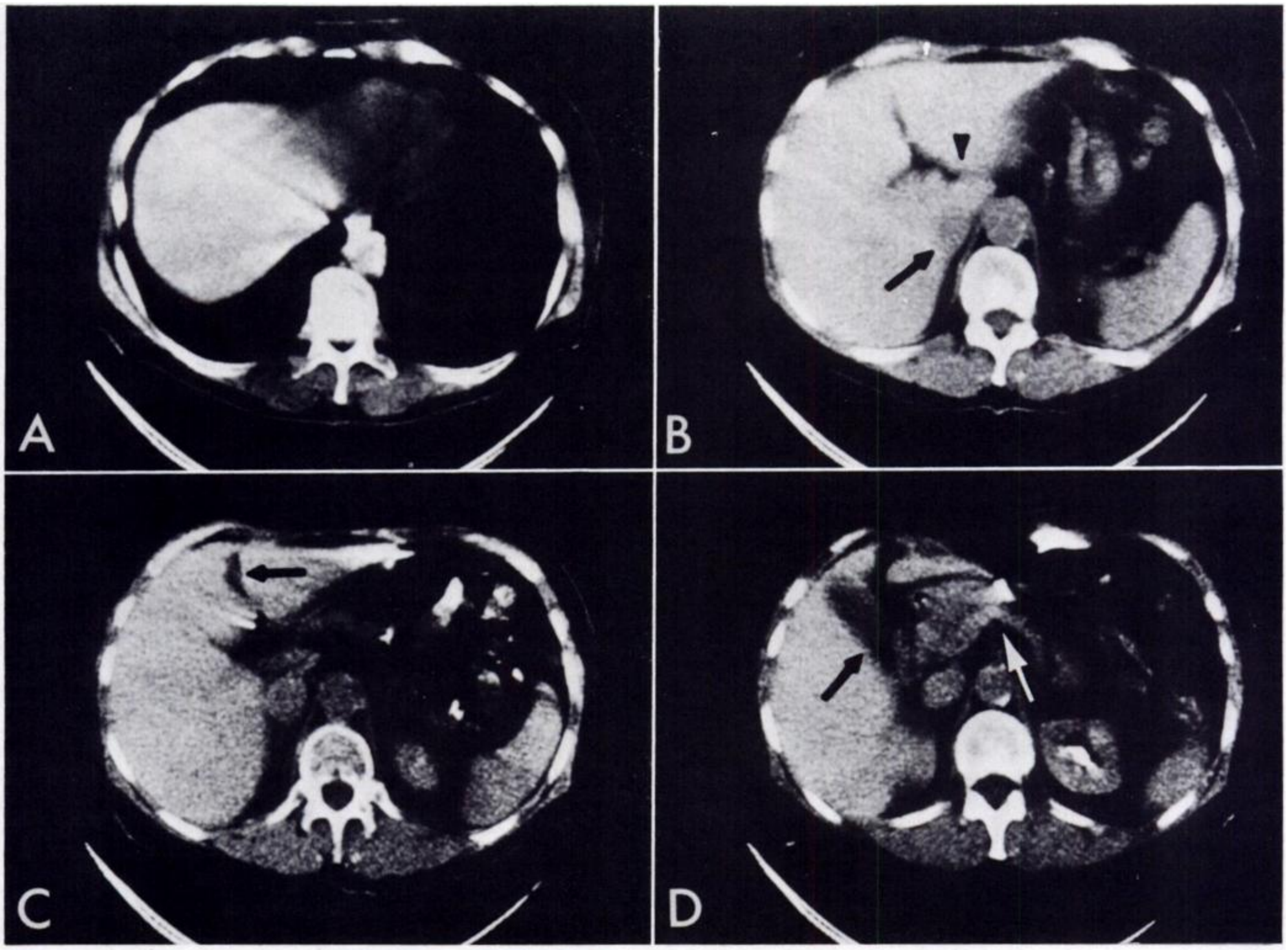

Fig. 1.—CT scans of normal liver. *A*, Uppermost scan showing dome of right lobe surrounded by lung. Streaklike artifacts caused by motion of heart, seen to left of liver. *B*, Scan at next level showing caudate lobe between fissure for ligamentum venosum (*arrowhead*) and inferior vena cava (*arrow*), which is within substance of liver. *C*, Scan at next level showing extrahepatic vena cava, quadrate lobe between fissure for falciform ligament and ligamentum teres (*arrow*), and gallbladder fossa, also seen at still lower level (*D*). *D*, Scan at lowest level showing gallbladder (*black arrow*) as low density structure on visceral surface of liver. Pancreas (*white arrow*), left kidney, and upper pole of right kidney also seen. Left renal collecting system opacified with previously administered contrast material.

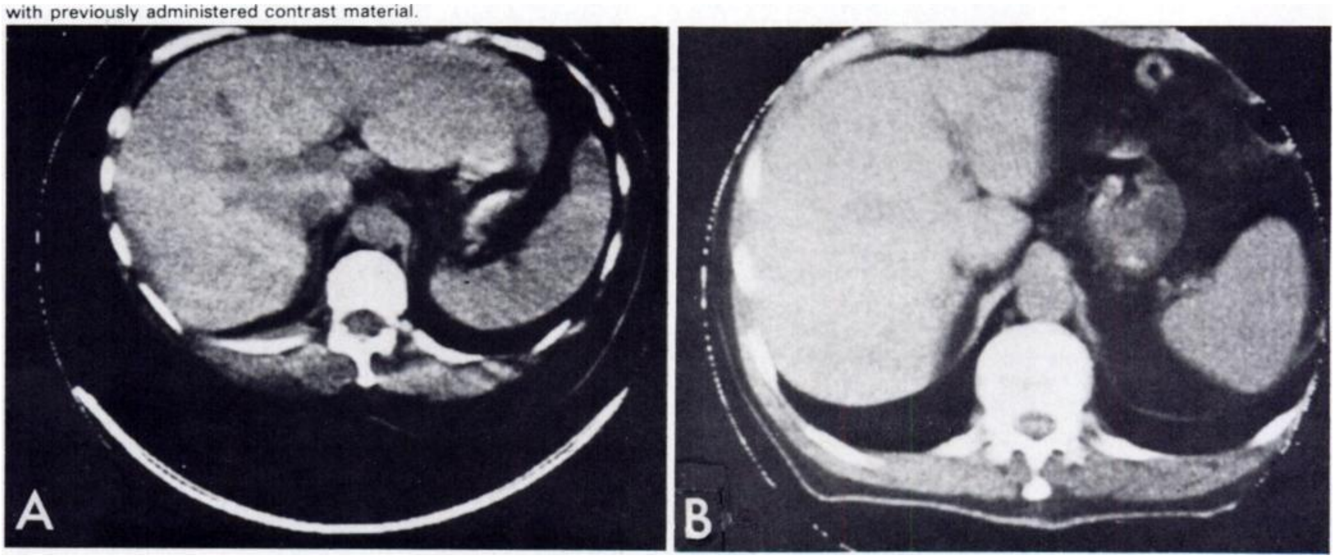

Fig. 2.—CT scans of two normal livers showing variation in size and shape of left hepatic lobe.

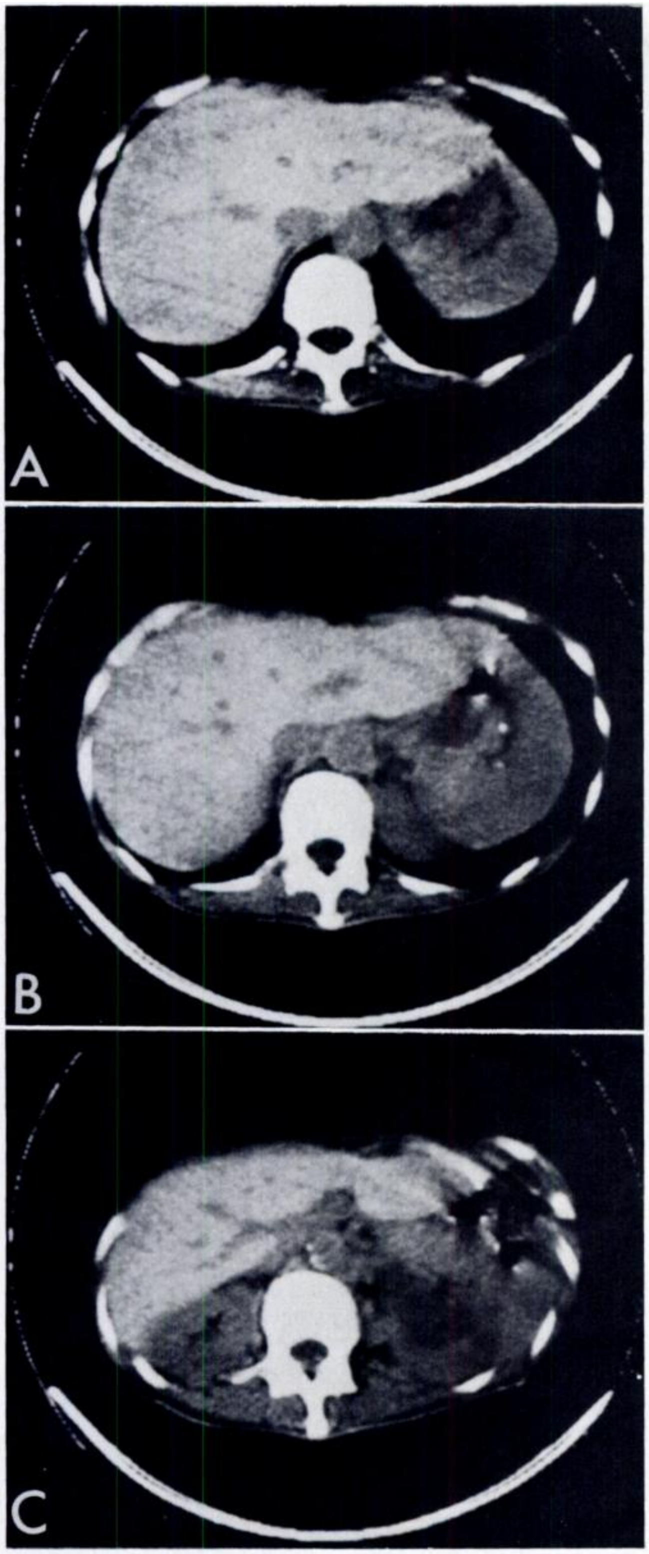

Fig. 3.—CT scans of normal liver with intrahepatic vessels. Portal tracts and vena cava are low density structures contrasting with higher density of parenchyma. In cross section (*A and B*), portal tracts are small round lucencies, but in left lobe (*B*) and toward hilum (*C*), linear and branching pattern is evident. Left kidney (*C*) is hydronephrotic because of distal ureteral obstruction.

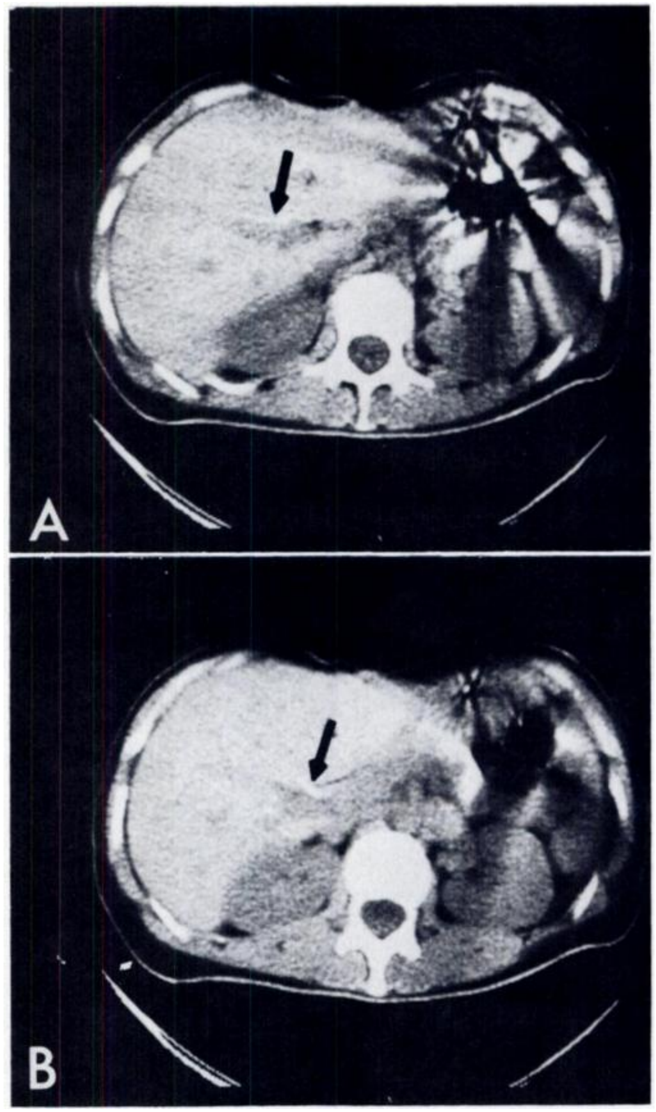

Fig. 4.—CT scans after administration of cholangiographic material showing that opacified bile ducts (*arrows*) are only very small part of radiolucent portal tracts. Artifacts caused by motion of gas in stomach.

blood, and thus the larger vessels will be seen as structures of lower density. The intrahepatic part of the inferior vena cava and larger portal branches are commonly identified. Further peripherally, especially in the right lobe, branches of the portal triad appear in cross section as small rounded radiolucencies that resemble focal lesions. However, as they converge toward the hilum and within the left lobe, their linear and branching pattern can be appreciated (fig. 3).

It has been recognized previously that intrahepatic bile ducts, because of the low density of bile, are readily apparent when they are dilated [1, 2, 4–9]. However, scans of the liver made after opacification of bile (fig. 4) and after opacification of blood (fig. 5) with contrast material show that it is the vascular components, and perhaps associated adipose and connective tissue, of the portal tracts that

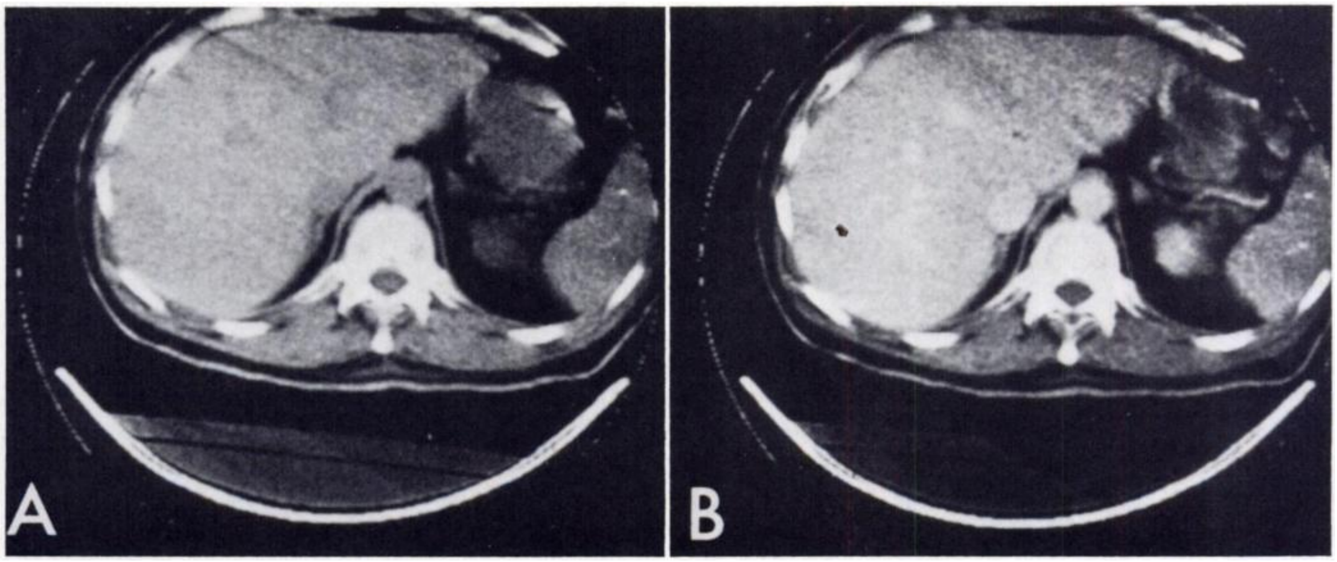

Fig. 5. — CT scans showing that small radiolucencies within liver on initial scan (*A*) are vessels since they become opaque after intravenous infusion of contrast material (*B*). Note also opacification of vena cava, aorta, and upper pole of left kidney.

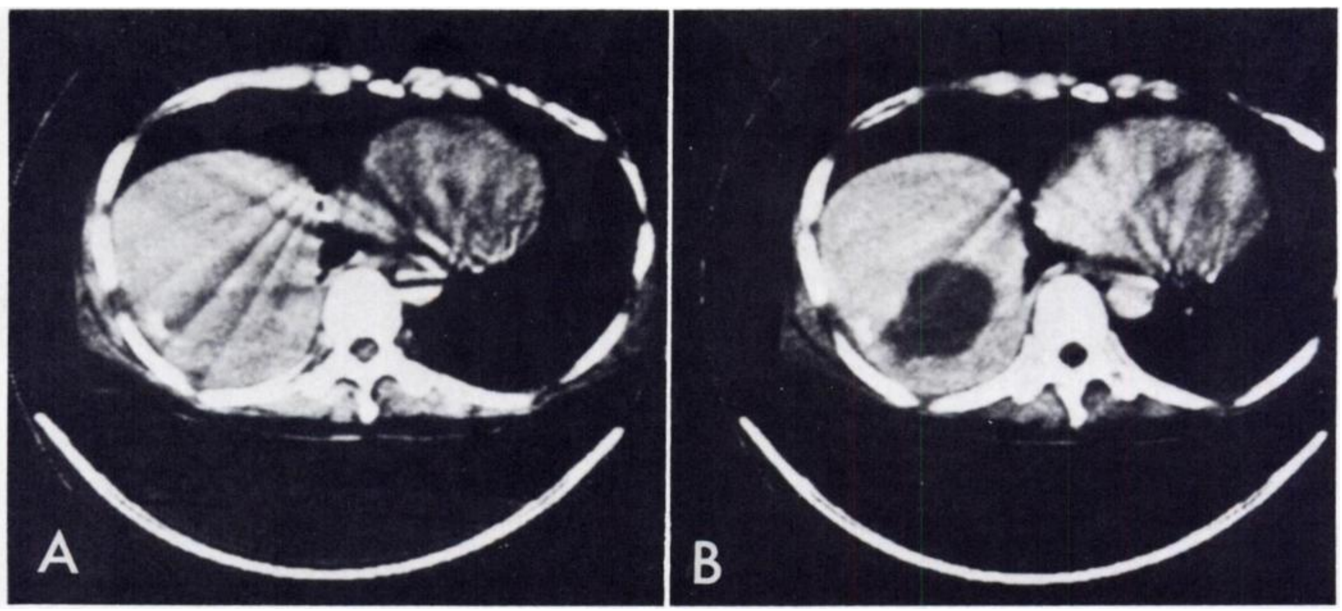

Fig. 6. — Pyogenic abscess in dome of right lobe. Lesion difficult to appreciate on initial scan (*A*) but becomes obvious after intravenous infusion of contrast material (*B*). Small opacity lateral to lesion is opaque drainage tube. Streak artifacts caused by cardiac motion.

contribute most to the radiolucent image of the normal portal triad.

Effect of contrast material. Intravenously administered iodinated contrast material increases the density of the liver. The opacification is related in general to the dose of iodine. It is also related to the timing of the scan relative to the administration of contrast material; scans made soon after infusion or injection show the greatest opacification. Evidence from recent experiments indicates that both intra- and extravascular concentrations of iodine contribute to the contrast enhancement [10].

In clinically acceptable doses, urographic contrast material provides much greater hepatic opacification than does cholangiographic material. We only used cholangiographic material to opacify bile ducts in a few cases early in our experience.

Artifacts and image degradation. Artifacts of a stellate or streaklike pattern emanate from materials of extremely high or low radiographic density, especially if there is motion during the scans (fig. 4) [11]. These may be superimposed over the liver image, but their artifactual nature is easily recognized, and although they can obscure a lesion, they are not likely to be mistaken for one.

Less obvious but more significant is the degradation of diagnostic quality that results from respiratory motion [12]. Suspension of breathing during the scan is essential to produce a technically superior CT examination, especially of the liver, because of its proximity to the diaphragm.

One form of biologic motion that cannot be suspended but often causes artifacts in scans of the dome of the liver is cardiac pulsation (figs. 1 and 6). Another problem some-

times encountered in scans of the uppermost part of the liver is apparent diminution of liver density caused by inclusion of overlying lung in the CT slice. An important principle in all CT interpretations is that the densities recorded in a CT reconstruction represent the attenuation of x-rays by all of the tissues within the volume of the CT slice. Unless a structure occupies the entire thickness (z axis) of a slice, the displayed densities of that structure also will include contributions from underlying and overlying material within the slice (see fig. 10).

Other forms of image degradation are caused by mechanical and technical problems in image production and reconstruction. The most common in our experience has been excessive noise, which is manifested as too much variation in image density from picture element to picture element. Because hepatic parenchyma is normally homogeneous, noise is especially noticeable in liver scans.

Mass Lesions

Space-occupying lesions within the liver are detectable by CT when their attenuation of the x-ray beam differs appreciably from the attenuation by the surrounding tissue. The great majority of all intrahepatic masses discovered, whether they are solid or cystic, neoplastic or inflammatory, are of diminished radiographic density. The exceptions we noted were lesions containing calcium or extravasated blood. Mass lesions that we have seen are listed in table 1.

The effect of intravenously administered contrast material on hepatic masses varies and probably depends more than anything else on the vascularity of the lesions. Avascular and relatively avascular masses (cysts, abscesses, and some neoplasms) become opacified either not at all or much less than the surrounding parenchyma, and thus their detection is enhanced (fig. 6). Some neoplasms that are apparent on scans made before administration of contrast material become less obvious or disappear afterward (fig. 7). This effect is probably due to the vascularity of the lesion and the chance performance of the scan when opacification of the parenchyma and the lesion are about equal. The highly vascular part of a cavernous hemangioma became denser than the normal parenchyma on a scan made immediately after infusion of a large dose [7].

A simpler method of varying contrast of an image is by manipulating the window settings on the viewing device. Narrowing the window increases the contrast between different densities and decreases the latitude of tissue densities displayed. Lesions that might be overlooked at one window setting may be obvious at another (fig. 8). To take advantage of the information present on a CT reconstruction, each scan must be viewed at various window settings.

Information provided by CT usually permits differentiation between cystic and solid lesions. Cysts are sharply demarcated, have thin walls, and are of a density near that of water (fig. 9). Solid tumors usually are not as well defined, and their density is intermediate between the densities of water and normal liver. As previously discussed, the apparent density of a lesion as recorded by CT may be misleading if normal tissue is also included in the same z axis of the CT slice (figs. 9*B* and 10). Also, a solid neoplasm can undergo cystic degeneration, a feature that we have noted among a few metastatic tumors (fig. 11).

TABLE 1

Mass Lesions of Liver Detected by CT

Lesion	No. Cases
Malignant neoplasms:	
Hepatoma	3
Hepatoblastoma	1
Metastases:	
Colon and rectum	8
Pancreas	8
Smooth muscle	3
Ovary	2
Lymphoma	2
Thyroid	1
Breast	1
Esophagus	1
Stomach	1
Small intestine	1
Kidney	1
Skeletal muscle	1
Melanoma	1
Unknown	10
Direct extension:	
Histiocytoma	1
Leiomyosarcoma	1
Hemangioendothelioma	1
Subtotal	48
Benign masses:	
Focal nodular hyperplasia	2
Hamartoma	1
Cavernous hemangioma	2
Cysts	3
Pyogenic abscess	2
Gunshot wound	1
Regenerative nodules	2
Subtotal	13
Total	61

We found only two uncalcified lesions that had components with densities greater than the density of normal liver. One was a metastatic adenocarcinoma from the colon (fig. 12) and the other was a gunshot injury (fig. 13). In both lesions, the increased density probably was caused by extravasated blood, a speculation that is supported by a previous in vitro study [3] and by the fact that we also saw increased density at the site of a recent needle biopsy.

The minimal size that a lesion can be and still be detected depends largely on the degree that its density varies from normal. Very tiny calcific deposits in the liver and collections of gas in the ducts may be obvious, whereas tumors of the same size would not be seen. Cysts and tumors no greater than 1 cm have been displayed, but at that size it

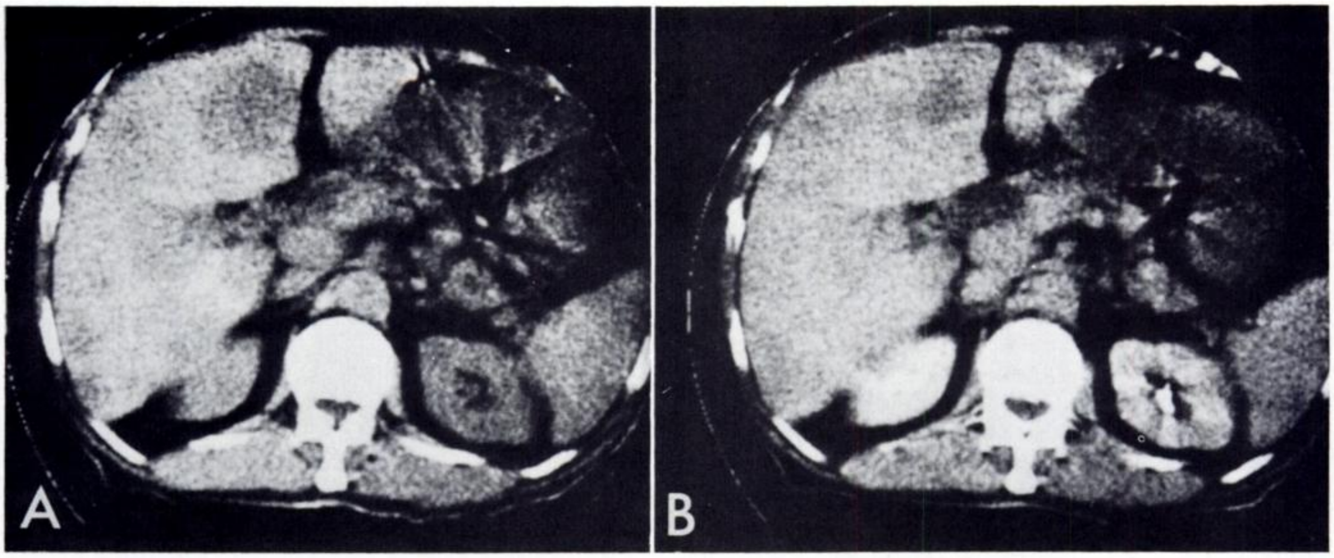

Fig. 7. — Metastatic adenocarcinoma from pancreas. Multiple mass lesions of diminished density more obvious on initial scan (*A*) than on scan at same level after administration of contrast medium (*B*).

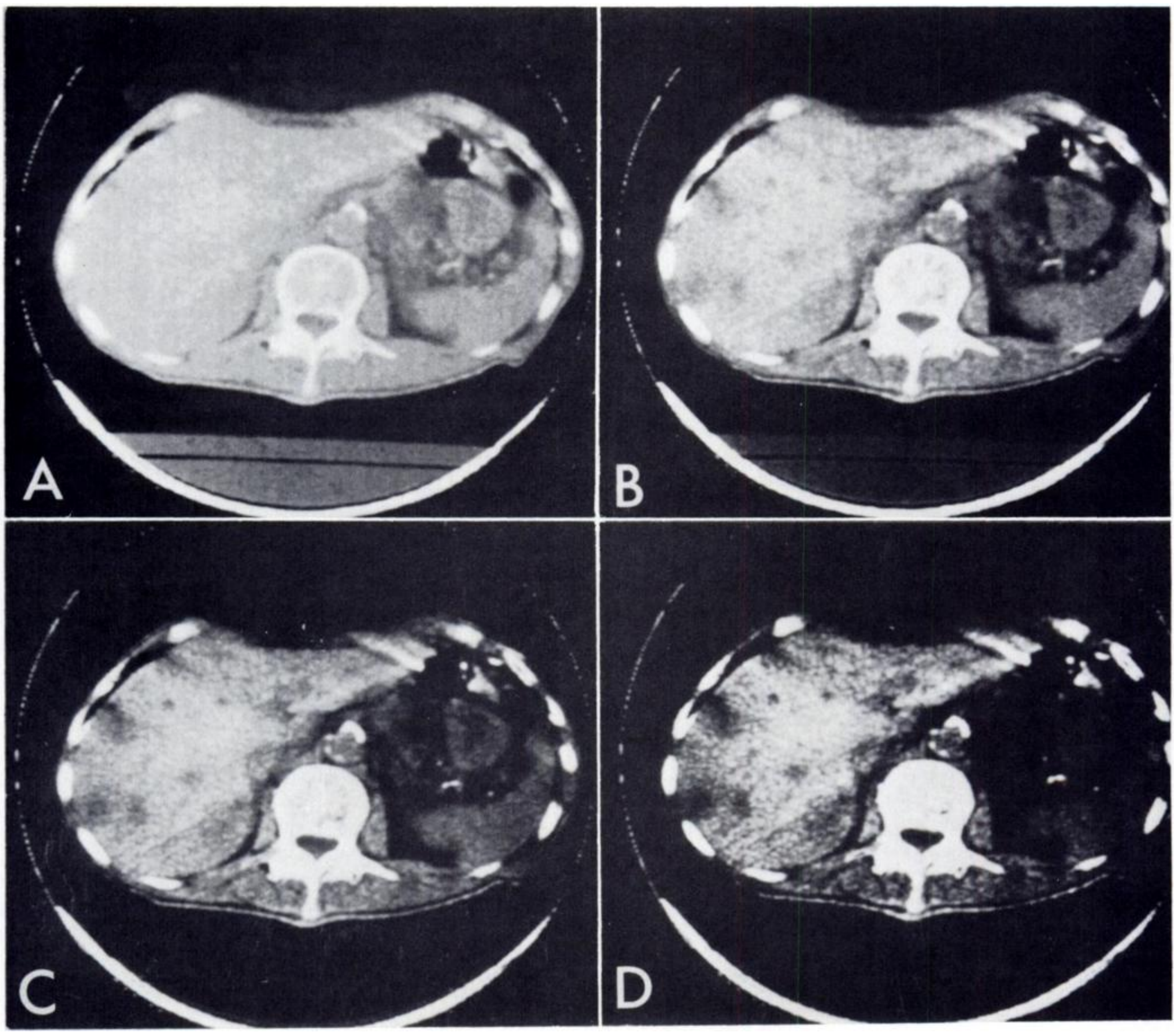

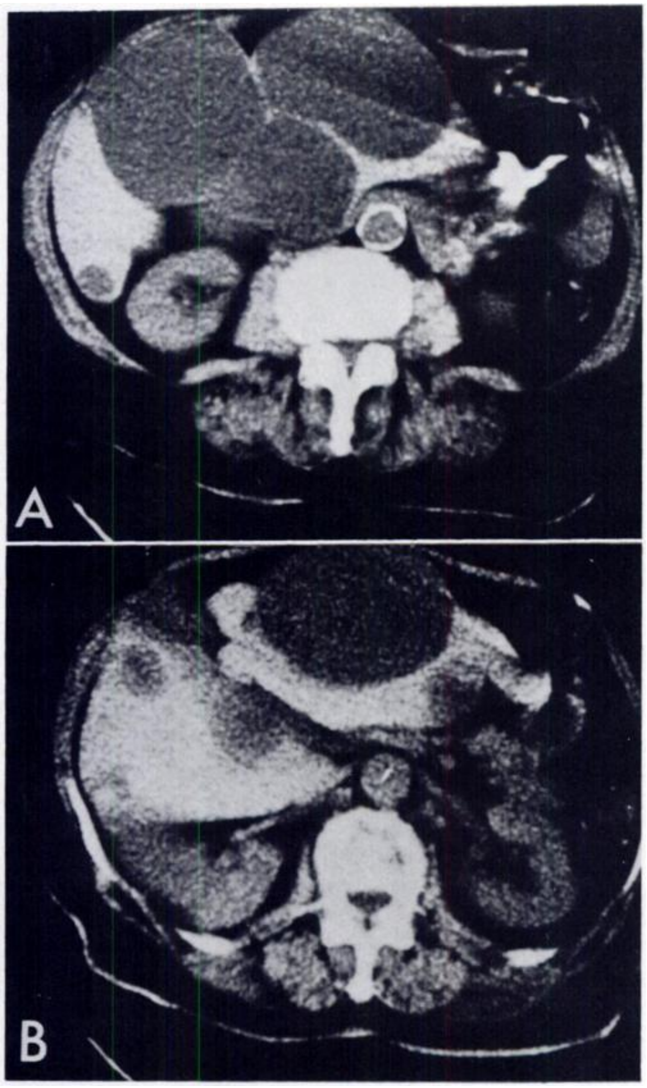

Fig. 9.—Polycystic liver. *A*, Scan at lower level showing cysts sharply marginated and of uniformly low density. Where they are approximated, thin cyst walls can be seen. *B*, Scan at higher level showing some cysts in right lobe with nonuniform density and poorly defined margins, probably because hepatic parenchyma also included in CT section (see fig. 10).

may not be possible to differentiate them from portal tracts.

Malignant neoplasms. With the exceptions previously mentioned, the radiographic density of most malignant tumors that we have detected has been between that of water and that of normal liver. The tumors are most apparent in livers that have a relatively high normal parenchymal density which provides a natural contrast. Some tumors have very subtle density differences and require manipulation of window settings for detection; others can be detected only after administration of contrast material (fig. 14).

In three patients who subsequently were found to have metastatic tumors, the entire liver appeared normal. In one patient with a huge hepatoma, massive liver enlargement only was noted, though minimal alteration in density was seen in retrospect [5]. Contrast material was not used in any of these patients. In some livers that contained multiple metastatic lesions, one or more of the several tumors subsequently found had escaped detection on CT. Lesions located in the dome of the liver near the diaphragmatic surface were especially difficult to detect.

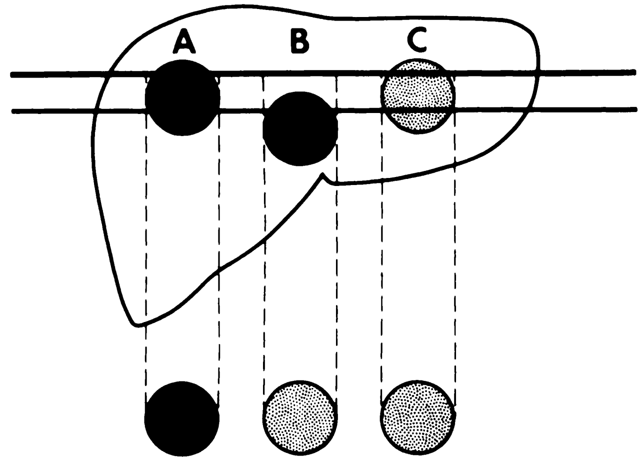

Fig. 10.—Effect of overlying tissue in *z* axis on recorded attenuation. Space between solid parallel lines represents thickness of CT scan (13 mm). Black circles (*A* and *B*) in liver represent spherical fluid-filled cysts of water density and gray circle (*C*), a solid tumor. Density (attenuation values) of lesions *A* and *C* accurately recorded on CT reconstruction because they occupy entire thickness of scan; density of lesion *B* inaccurately recorded as identical to solid lesion because overlying hepatic parenchyma in scan contributes to attenuation.

Despite the variety of neoplasms studied, there is little evidence to suggest that the histologic type, site, or origin of a tumor can be predicted on the basis of CT appearance. Perhaps further experience will show that some of the information provided by CT, such as response of a lesion to contrast material or its unusual density, will be characteristic of certain tumor types. The hepatomas in our series had minimal alterations of density, but other investigators [1, 2] have reported hepatomas of substantially diminished density. The two lymphomas could not be distinguished from other neoplasms.

One benefit of abdominal CT is that the information provided is not limited to a single organ. Previously undiagnosed primary malignant lesions in the pancreas (fig. 11) and kidney (fig. 15) have been found in examinations that were done primarily to investigate the liver. Likewise, clinically unsuspected hepatic metastases have been discovered in CT investigations of other suspected conditions.

The malignant lesions that involved the liver by direct extension were large tumors of multiple abdominal struc-

←

Fig. 8.—Single CT scan of patient with metastatic esophageal carcinoma showing effect of window width. *A*, Widest setting showing greatest latitude of densities but barely perceptible lesions. *B–D*, Successively narrower settings showing increased contrast and more obvious hepatic lesions but diminished range of densities.

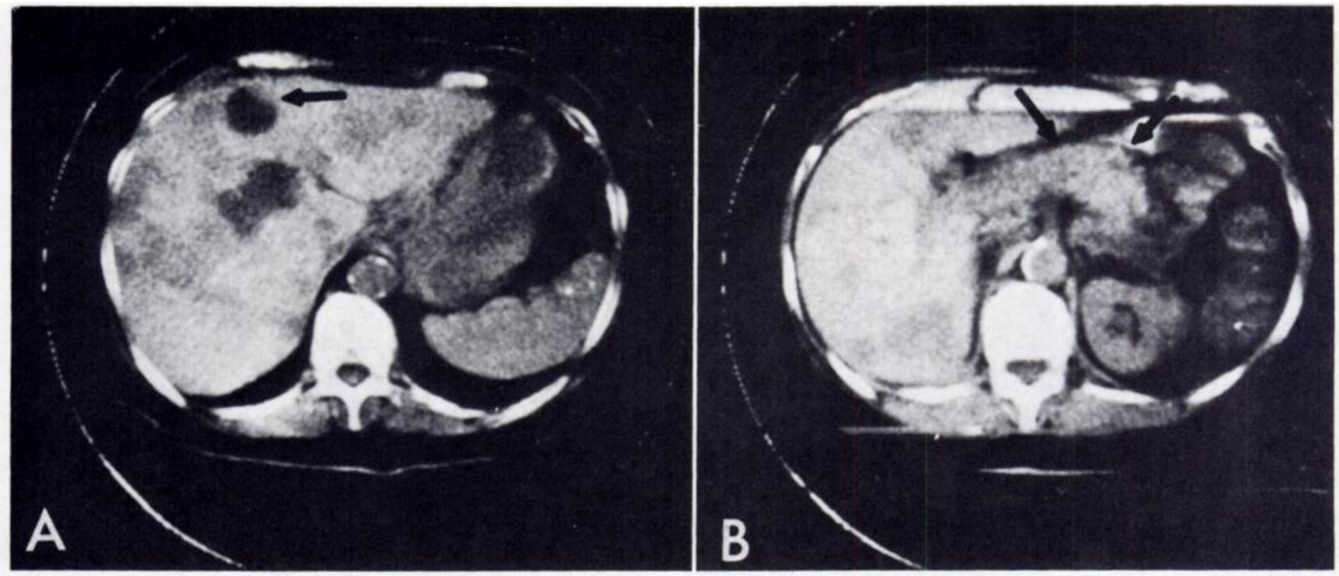

Fig. 11.—CT scans showing metastasis from carcinoma of pancreas with metastatic lesions throughout liver. *A*, Two lesions with very low density, probably a result of cystic degeneration, one seems to have mural nodule (*arrow*). *B*, Primary tumor in body and tail of pancreas (*arrows*).

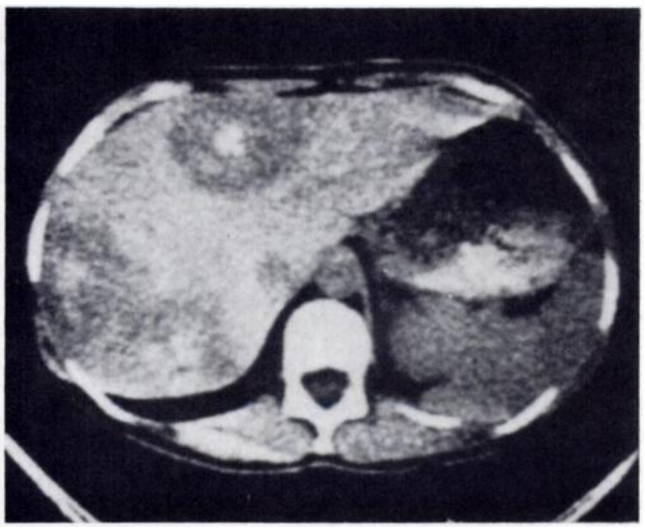

Fig. 12.—CT scan showing metastatic adenocarcinoma from colon. Central foci of increased density within predominately low density metastatic tumors believed to be blood within areas of necrosis. Dense material in stomach probably caused by ingested meat.

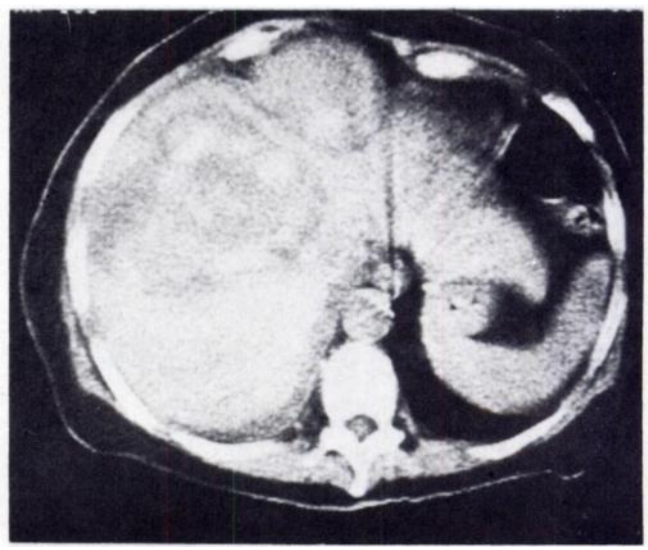

Fig. 13.—CT scan showing extent of hepatic damage caused by bullet that penetrated liver from thorax. Areas of increased density within large low density lesion probably blood. Somewhat localized mass anteriorly may be subcapsular collection. Patient recovered without surgical intervention.

tures. The malignant histiocytoma and the hemangioendothelioma (fig. 16) both had extensive calcific deposits. The leiomyosarcoma, which apparently originated in the retroperitoneum, had undergone cystic degeneration.

Benign masses. Although a diverse group of benign space-occupying lesions was demonstrated (table 1), our experience in any one of these conditions is limited. While we have not studied a benign hepatic adenoma, Sagel et al. [4] illustrated a large adenoma that was visible as a lesion of diminished density after administration of contrast material. We have seen focal nodular hyperplasia as a lesion of slightly diminished density, which in one case altered the hepatic contour [5]. The vascular periphery of one of the two cavernous hemangiomas became densely opacified with contrast infusion [7]. The other hemangioma was a large lesion, most of which was perceptible only after injection of contrast medium. Septa could be seen within a cystic hamartoma (fig. 17). Of the two pyogenic abscesses, one was obvious on initial scans as a low density lesion, while the other (fig. 6) was best seen after contrast enhancement.

Diffuse Liver Disease

In the nine patients with clinically apparent cirrhosis, no outstanding alteration in hepatic density was seen on CT, although in two the liver parenchyma had a slight nonspecific inhomogeneity. Ascites, not always evident clin-

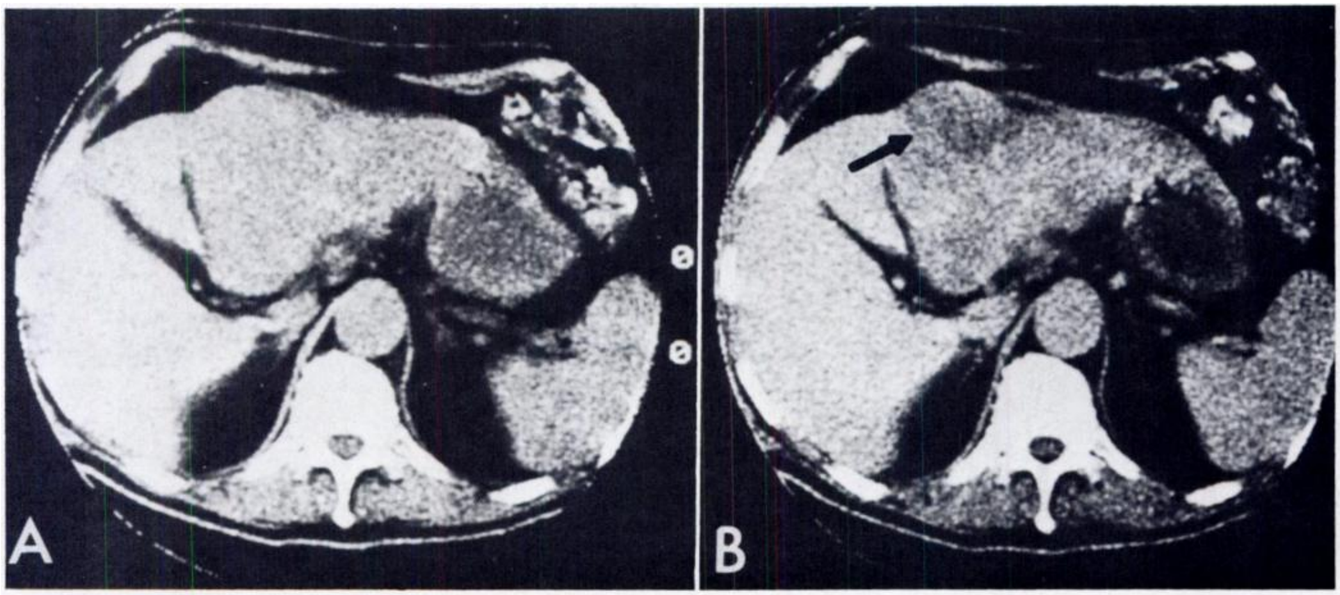

Fig. 14.—Metastatic carcinoma from rectum. *A*, Initial scan showing generally diminished density and anterior bulge in left lobe of uncertain significance. *B*, Scan after administration of contrast material showing lesion more definitely (*arrow*).

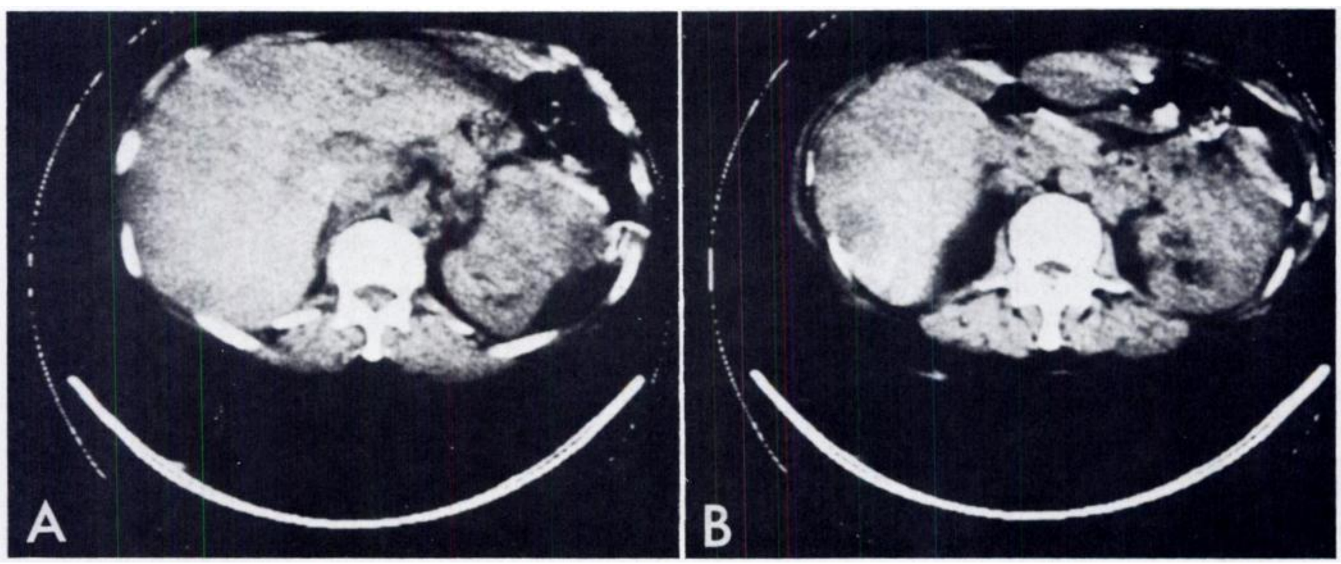

Fig. 15.—CT scans showing hepatic metastasis from renal carcinoma. Discovered during CT evaluation of suspected hepatic abscess. Multiple mass lesions in liver typical of metastasis; large mass arising from anterior aspect of left kidney characteristic of renal cell carcinoma. Note inhomogeneous density of renal tumor and absence of well defined interface with renal parenchyma.

ically, was present in six patients, three of whom also had splenomegaly. Two patients had gross surface nodularity, which on peritoneoscopy was found to be regenerative nodularity.

The diffuse process with the most impressive CT appearance was fatty infiltration, a finding noted in five patients. In this condition, the diminished parenchymal density is easily recognized by comparing it with the density of the spleen (fig. 18). The intrahepatic vessels stand out as relatively dense structures against the radiolucent background of hepatic parenchyma.

Only one of our five patients with fatty liver admitted to alcohol abuse, although one had a history of chronic recurrent pancreatitis. The other three patients all had diabetes. None of the patients with fatty liver had clinical evidence of liver impairment, and laboratory evidence was either lacking or marginal.

Dilated Intrahepatic Bile Ducts

The value of CT as a noninvasive method of detecting biliary obstruction is already well recognized [2, 4–8]. We did not systematically investigate the ability of CT to differentiate between obstructive and nonobstructive jaundice, but we did find dilated intrahepatic ducts in 13 patients with subsequently proved biliary obstruction. Segmental dilatation of intrahepatic ducts was seen in one

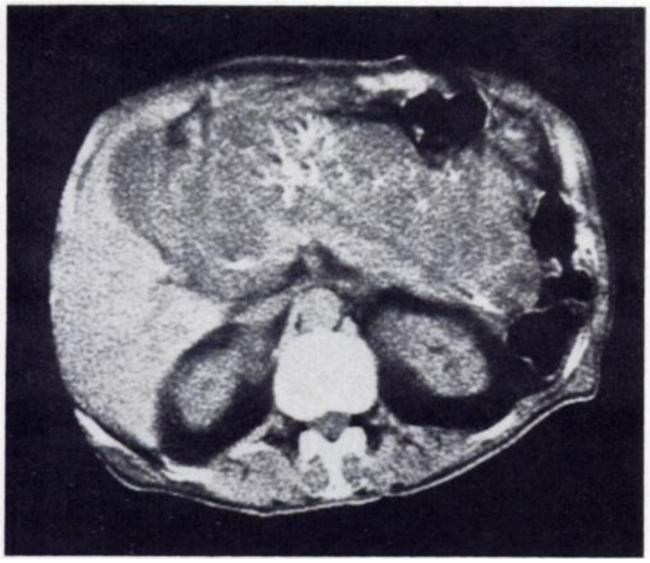

Fig. 16.—Hemangioendothelioma in patient with von Hippel-Lindau's disease. Large inoperable tumor involves liver, pancreas, and kidneys. Calcific deposits present within mass.

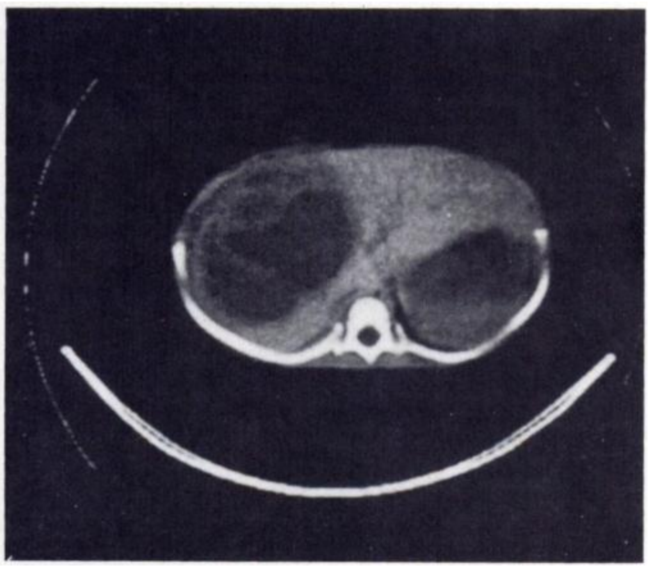

Fig. 17.—Cystic hamartoma in 6-month-old child. Septa in cystic lesion occupies most of right hepatic lobe.

nonobstructive condition (Caroli's disease).

In most most patients, the dilated ducts were easily recognized because of the low density of bile. These ducts should not be confused with normal portal veins, which have the same distribution but which are somewhat denser. If there is doubt, administration of urographic contrast material diminishes the contrast between parenchyma and portal vein, but accentuates the contrast between parenchyma and dilated ducts.

An attractive feature of CT in evaluation of biliary obstruction is that information about the obstructing lesion often is obtained. Masses in the porta hepatis (fig. 19) and head of the pancreas were found in seven of the 13 patients with dilated ducts. In two other patients, the

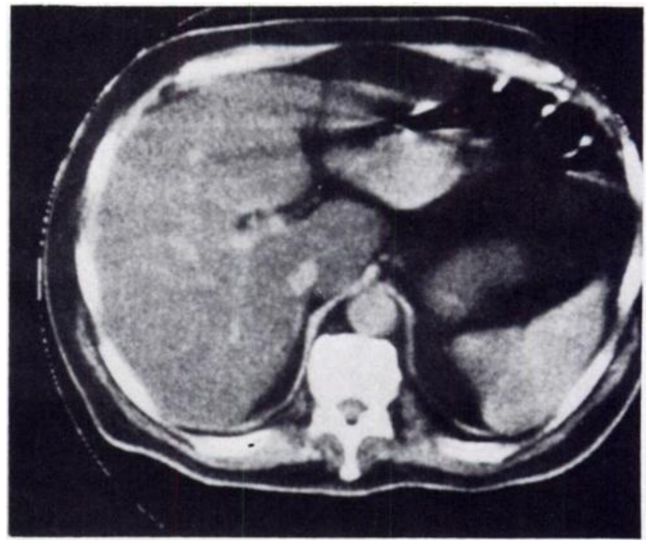

Fig. 18.—Fatty infiltration in diabetic patient without clinical evidence of liver impairment. Density of hepatic parenchyma less than that of normal spleen. Vena cava and portal tracts stand out as relatively dense structures against radiolucent hepatic parenchyma.

presence of a dilated pancreatic duct associated with dilated bile ducts established the site of obstruction as beyond the confluence of the common bile duct and pancreatic duct. At surgery, both patients were found to have small carcinomas of the ampulla of Vater.

Discussion

Since the first published CT image of the liver in 1975 [13], remarkable technologic advancements have permitted CT to develop into a clinically valuable diagnostic method capable of providing unique information about the liver. CT has been especially helpful in evaluating known or suspected space-occupying lesions and biliary tract obstruction. So far it has been of limited value in diffuse nonneoplastic hepatic disease, except for fatty infiltration.

The proper clinical role of CT in relation to other diagnostic methods, especially nuclear imaging, remains to be established. Other investigators have addressed this problem [2], and the results of our own initial experience in comparing the accuracy of the two methods is the subject of another study recently completed [14].

Both CT and radionuclide scanning are highly accurate methods of detecting mass lesions. Because the images are produced by different means, the information provided is of a different nature and is often complementary rather than competitive. In some cases, masses suspected by equivocal findings on one of the procedures have been confirmed by the other. In general, CT offers more specific information about the composition of a mass and has a greater ability to differentiate between lesions and anatomic variants [2, 6, 14]. Since both methods are still evolving, their relative value in detecting hepatic masses in a particular clinical setting may depend on the equipment and experience available.

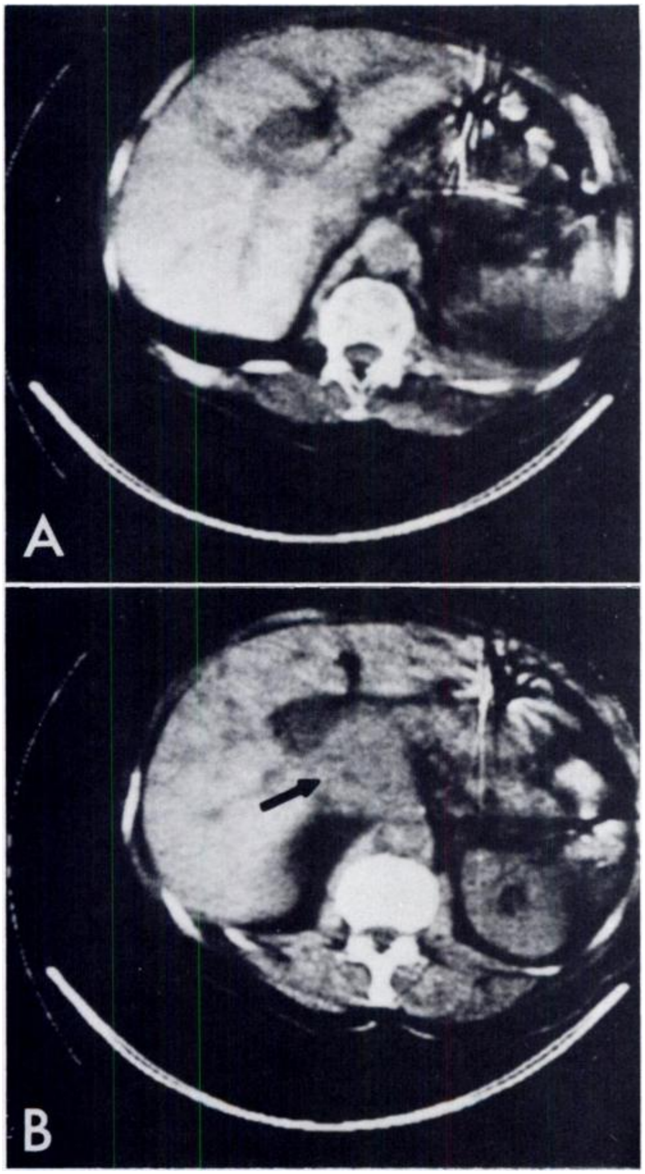

Fig. 19.—Biliary obstruction. Dilated branching bile ducts seen throughout liver, and obstructing mass (metastatic bronchogenic carcinoma) apparent near hilum of liver (*arrow*). Poor technical quality partly due to patient's inability to suspend respiration during scans.

Nuclear imaging, because it somewhat reflects liver function, is clearly superior in evaluating most diffuse liver disease, but CT can add additional information and is especially sensitive to fatty infiltration. CT is superior in detecting biliary ectasia and often defines the obstructing lesion [2, 6, 14].

Abdominal CT is not limited to a single organ or system, and each examination provides diagnostic information about multiple structures. As previously illustrated, hepatic lesions have been found on investigations requested primarily to evaluate other organs; likewise, significant lesions have been found in other organs on examinations designed primarily to investigate the liver. The most common examination done with our body scanning unit is a study of the upper abdomen that includes liver, pancreas, kidneys, adrenal glands, and a considerable part of the retroperitoneum.

Experience has convinced us of the importance of direct professional supervision of abdominal CT examinations, with each study tailored according to the clinical problem and the CT findings. Ideally, all scans should be viewed before the examination is terminated. Anticipated further reduction in processing time will allow more convenient monitoring of the examination, reduce examination time, and increase the daily capacity of the scanning unit for patient examinations.

The importance of a scan time that is rapid enough to permit the patient to suspend respiration has been discussed. Although scans of the liver made with patients breathing have produced some impressive results [2], many of the more subtle findings can be displayed only on scans free of degradation by respiratory motion.

Investigators at the Cleveland Clinic have taken advantage of their scanning facility to perform precise needle placements in the liver for biopsy and aspiration of lesions [1, 2] and, in at least one case, to insert a drainage catheter for treatment of an abscess [15]. While we have not yet used CT for those purposes, the advantages of a guided approach are readily apparent.

Like any diagnostic radiologic procedure, CT provides information that is subject to interpretation, and its diagnostic accuracy depends on the knowledge and experience of the interpreter. Much remains to be learned about CT of the liver, and important information should be forthcoming as clinical investigation becomes more widespread.

REFERENCES

1. Alfidi RJ, Haaga J, Meaney TF, MacIntyre WJ, Gonzales L, Tarar R, Zelch MG, Boller M, Cook SA, Jelden G: Computed tomography of the thorax and abdomen: a preliminary report. *Radiology* 117:257–264, 1975
2. Alfidi RJ, Haaga JR, Havrilla TR, Pepe RG, Cook SA: Computed tomography of the liver. *Am J Roentgenol* 127: 69–74, 1976
3. Philips RL, Stephens DH: Computed tomography of liver specimens. *Radiology* 115:43–46, 1975
4. Sagel SS, Stanley RJ, Evens RG: Early clinical experience with motionless whole-body computed tomography. *Radiology* 119:321–330, 1976
5. Sheedy PF II, Stephens DH, Hattery RR, Muhm JR, Hartman GW: Computed tomography of the body: initial clinical trial with the EMI prototype. *Am J Roentgenol* 127:23–51, 1976
6. Stanley RJ, Sagel SS, Levitt RG: Computed tomography of the body: early trends in application and accuracy of the method. *Am J Roentgenol* 127:53–67, 1976
7. Stephens DH, Hattery RR, Sheedy PF II: Computed tomography of the abdomen: early experience with the EMI body scanner. *Radiology* 119:331–335, 1976
8. Stephens DH, Sheedy PF II, Hattery RR, Hartman GW: Initial clinical experience with computerized tomography of the body. *Radiol Clin North Am* 14:149–158, 1976
9. Michels NA: Newer anatomy of the liver and its variant blood

supply and collateral circulation. *Am J Surg* 112:337–347, 1966
10. Kormano M, Dean PB: Extravascular contrast material: the major component of contrast enhancement. *Radiology* 121:379–382, 1976
11. McCullough EC, Payne JT, Baker HL Jr, Hattery RR, Sheedy PF, Stephens DH, Gedgaudus E: Performance evaluation and quality assurance of computed tomography scanners, with illustrations from the EMI, ACTA, and Delta scanners. *Radiology* 120:173–188, 1976
12. Alfidi RJ, MacIntyre WJ, Haaga JR: The effects of biological motion on CT resolution. *Am J Roentgenol* 127:11–15, 1976
13. Schellinger D, Di Chiro G, Axelbaum SP, Twigg HL, Ledley RS: Early clinical experience with the ACTA scanner. *Radiology* 114:257–261, 1975
14. MacCarty RL, Wahner H, Stephens DH, Sheedy PF II, Hattery RR: A retrospective comparison of radionuclide scans and computerized tomography of the liver and pancreas. Submitted for publication
15. Haaga JR, Alfidi RJ, Cooperman AM, Havrilla T, Meaney TF, Ockner SA, Stiff P, Silver S: Definitive treatment of a large pyogenic liver abscess with CT guidance. *Cleve Clin Q* 43:85–88, 1976